GeroScience (2024) 46:4689–4706
https://doi.org/10.1007/s11357-024-01207-y

ORIGINAL ARTICLE

Fmo induction as a tool to screen for pro-longevity drugs

Shijiao Huang · Rebecca L. Cox · Angela Tuckowski · Safa Beydoun · Ajay Bhat · Marshall B. Howington · Marjana Sarker · Hillary Miller · Ethan Ruwe · Emily Wang · Xinna Li · Emily A. Gardea · Destiny DeNicola · William Peterson · Jeffrey M. Carrier · Richard A. Miller · George L. Sutphin · Scott F. Leiser

Received: 19 March 2024 / Accepted: 15 May 2024 / Published online: 24 May 2024
© The Author(s), under exclusive licence to American Aging Association 2024

Abstract Dietary restriction (DR) and hypoxia (low oxygen) extend lifespan in *Caenorhabditis elegans* through the induction of a convergent downstream longevity gene, *fmo-2*. Flavin-containing monooxygenases (FMOs) are highly conserved xenobiotic-metabolizing enzymes with a clear role in promoting longevity in nematodes and a plausible similar role in mammals. This makes them an attractive potential target of small molecule drugs to stimulate the health-promoting effects of longevity pathways. Here, we utilize an *fmo-2* fluorescent transcriptional reporter in *C. elegans* to screen a set of 80 compounds previously shown to improve stress resistance in mouse fibroblasts. Our data show that 19 compounds significantly induce *fmo-2*, and 10 of the compounds induce *fmo-2* more than twofold. Interestingly, 9 of the 10 high *fmo-2* inducers also extend lifespan in *C. elegans*. Two of these drugs, mitochondrial respiration chain complex inhibitors, interact with the hypoxia pathway to induce *fmo-2*, whereas two dopamine receptor type 2 (DRD2) antagonists interact with the DR pathway to induce *fmo-2*, indicating that dopamine signaling is involved in DR-mediated *fmo-2* induction. Together, our data identify nine drugs that each (1) increase stress resistance in mouse fibroblasts, (2) induce *fmo-2* in *C. elegans*, and (3) extend nematode lifespan, some through known longevity pathways. These results define *fmo-2* induction as a

Supplementary Information The online version contains supplementary material available at https://doi.org/10.1007/s11357-024-01207-y.

S. Huang (✉) · R. L. Cox · S. Beydoun · A. Bhat · M. Sarker · H. Miller · E. Ruwe · E. Wang · S. F. Leiser (✉)
Molecular and Integrative Physiology, University of Michigan, Ann Arbor, MI 48109, USA
e-mail: shijiaoh@ksu.edu

S. F. Leiser
e-mail: leiser@umich.edu

A. Tuckowski · M. B. Howington
Cell and Molecular Biology Program, University of Michigan, Ann Arbor, MI 48109, USA

X. Li · R. A. Miller
Department of Pathology, University of Michigan School of Medicine, Ann Arbor, MI 316048109-2200, USA

E. A. Gardea · D. DeNicola · W. Peterson · J. M. Carrier · G. L. Sutphin
Department of Molecular & Cellular Biology, University of Arizona, Tucson, AZ 85721, USA

R. A. Miller
University of Michigan Geriatrics Center, Ann Arbor, MI 48109, USA

S. F. Leiser
Department of Internal Medicine, University of Michigan, Ann Arbor, MI 48109, USA

viable approach to identifying and understanding mechanisms of putative longevity compounds.

Keywords Flavin-containing monooxygenases · Hypoxia · Dietary restriction · *Fmo-2* induction · Longevity · Drugs · *C. elegans*

Introduction

Aging is the leading cause of many chronic diseases, and thus, the study of aging and longevity has applications across diverse research areas. Multiple longevity pathways have been identified to extend lifespan across species from yeast to mammals [1]. A primary goal of geroscience is to translate longevity studies in model organisms toward human health improvement. One way to accomplish this is through feasible interventions with small molecules that can be further developed and approved as preventive medications. Studies in mice show that small molecules such as rapamycin, acarbose, and 17α-estradiol extend mouse lifespan and healthspan [2–5]. These findings prove that small molecules can extend lifespan and improve health in mammals. However, studies of drug effects on mouse lifespan are costly and time-consuming. Some studies have performed small molecule screening for lifespan extension in short-lived model organisms. A pharmacological screen of 1280 compounds identified 60 drugs that can extend lifespan in *Caenorhabditis elegans* in liquid culture, and 33 of these 60 also increased stress resistance [6]. An FDA-drug repurposing study modelled drug candidates as binding partners of longevity genes and identified 29 drugs from 1347 FDA-approved drugs; 3 of the drugs were confirmed to extend lifespan in rotifers [7]. Another study showed that drug combinations can extend healthy lifespan synergistically by targeting multiple longevity pathways [8]. While each of these studies identified lifespan extending compounds, they also required extensive effort and had a relatively low "hit rate."

Combining screening for antiaging small molecules in both mammalian cells and *C. elegans* is a plausible approach to identify the conserved benefits of drugs that improve health. A recent study reported a high-throughput screening of 6351 compounds for increasing stress resistance in mouse fibroblasts and identified 75 compounds that either provided exceptionally strong protection from paraquat or were in the top 10% for resistance to paraquat and to either cadmium, methyl methanesulfonate (MMS), or both. Two of these compounds were shown to increase stress resistance through Nrf2/SKN-1 signaling [9]. Seventy of this set of 75 were tested for lifespan extension at 2 doses in *C. elegans* and 1 dose in *Drosophila melanogaster* for lifespan extension [9]. Doses were selected based on prior studies of other drugs. However, compounds tested were not enriched for lifespan extension of *C. elegans* or fly lifespan. Lombard et al. then took advantage of the fact that one of the libraries in their primary screen had previously been assayed for effects on worm lifespan in liquid culture by *Ye et al.* [6]. Using a much better-powered comparison, they were able to identify a relationship between the stress-resistant drug hits with lifespan extension in *C. elegans* [9]. In this study, we leverage those 75 compounds plus 5 additional stress-resistant drug hits from Lombard et al. to identify their role in Fmo induction and aging. We utilize induction of the longevity gene *fmo-2* as a pro-longevity marker and test lifespan of *C. elegans* treated by *fmo-2*-inducing small molecules on agar plates.

We previously found that *fmo-2* (*f*lavin-containing *m*ono*o*xygenase-*2*) is induced by and is a convergent downstream target of two longevity pathways (hypoxia and DR) in *C. elegans* [10]. Activation of the hypoxic response extends lifespan in *C. elegans*. The hypoxia-inducible factor-1 (HIF-1) transcription factor, which is stabilized under hypoxia, is well-conserved across species. The effects of HIF-1 stabilization are multi-faceted. HIF-1 stabilization by hypoxia, or loss-of-function mutations in the HIF-1 E3 ligase VHL produce longevity benefits in *C. elegans* [10], while VHL mutations in humans cause von Hippel-Lindau disease (VHL) [11]. *fmo-2* is induced and necessary for longevity downstream of hypoxia or stabilized HIF-1 in C. *elegans* [10]. Dietary restriction (DR) is the most well-studied and conserved longevity pathway from yeast to humans [1], but implementing long-term DR is not realistic in humans, because of both lack of compliance and potential drawbacks including low body weight and malnutrition. Strikingly, unlike the trade-off effects of hypoxia and DR, *fmo-2* overexpression in *C. elegans* causes no obvious negative effects while extending lifespan and improving healthspan [10]. A gene whose expression and/or activity is both necessary and sufficient to

robustly improve longevity in one or more pathways can serve as a longevity gene marker. Since *fmo-2* is both necessary and sufficient to increase lifespan downstream of multiple longevity pathways including DR and hypoxia, it makes *fmo-2* an ideal candidate longevity gene marker.

Fmos are highly conserved xenobiotic-metabolizing enzymes that oxygenate substrates by adding a molecule of oxygen to soft-nucleophilic atoms for detoxification in liver, kidney, and intestine in mammals. There are five Fmos in mammals, and five Fmos, arbitrarily numbered as *fmo-1* to *fmo-5*, in the *C. elegans* genome. Overexpression of *fmo-2* in *C. elegans* is sufficient to extend lifespan and improve stress resistance [10]. Work in *C. elegans*, *D. melanogaster*, and mice has demonstrated that long-lived animals or their cells are more resistant to multiple stresses [12–14]. A strong correlation between the maximum lifespan of different species and the stress resistance of their cells has also been observed [15]. Our previous work demonstrates that overexpression of mouse Fmos increases resistance to oxidative stress of paraquat or resistance to cadmium in both kidney and liver cells [16]. In mice, multiple Fmos are upregulated under longevity interventions including dietary restriction, disruption of growth hormone/insulin-like growth factor 1 (GH/IGF1) signaling, and rapamycin treatment [17, 18]. These results are consistent with a conserved role for Fmos in promoting health and longevity benefits in *C. elegans* and mammals. Thus, Fmo could be an important, conserved downstream longevity gene that provides beneficial aspects of hypoxia and/or DR. Further, induction of Fmo could be indicative of a hypoxia and/or DR mimetic if it can be induced without detrimental side effects. Additionally, drugs identified to act in the hypoxia or DR-mediated pathways of Fmo induction can improve the mechanistic understanding of the longevity pathways themselves.

Here, we perform a biased screen of drug hits that improve stress resistance in mouse fibroblasts [9] for induction of the longevity gene Fmo. Our results suggest that Fmo is commonly induced by stress resistance-inducing drugs in both mouse fibroblasts and *C. elegans*. In addition, *fmo-2* induction is a remarkably accurate predictor of drug-induced lifespan extension in *C. elegans*. By combining the *fmo-2* inducers with hypoxia or DR, we also pinpoint likely pathways of a subset of these small molecules for lifespan extension.

Results

Small molecules that improve stress resistance induce the Fmo longevity gene in both mice and *C. elegans*

A high-throughput screen of 6351 compounds identified drug hits that improve stress resistance in mouse fibroblasts [9]. To test the potential of these drug hits for their effects on longevity, we examined the expression of Fmo genes in the fibroblasts of genetically heterogeneous mice (UM-HET3) after drug treatment. Low, medium, and high doses (0.25, 1, or 4 μM) of each drug were used to treat the fibroblasts, and Fmo4 or Fmo5 mRNA level was measured. At the high drug dose, roughly one-third of the drugs (26 for *Fmo4* and 30 for *Fmo5*) significantly increased *Fmo4* or *Fmo5* mRNA levels more than 1.5-fold (Fig. 1A–D**;** Supplementary Table 1). Among these, 19 drugs induced both *Fmo4* and *Fmo5* (Fig. 1A and C; Fig. 1E; Supplementary Table 1). Across different doses of these 80 drugs, 52 increased either *Fmo4* or *Fmo5* expression significantly under at least one dose (Supplementary Table 6). More than 10% of the drugs (12 drugs for *Fmo4* and 8 for *Fmo5*) increased Fmo expression significantly at all three doses (Fig. S1**A**–**L**; Supplementary Table 1). Additionally, four compounds (butaclamol, carvedilol, phenelzine, and vortioxetine) increased *Fmo4* expression, and five compounds (AEG3482, cannabidiol, PNU-74654, SKF 83959 hydrobromide, sodium nitroprusside) increased *Fmo5* expression at all three doses more than 1.5-fold but were not statistically significant. While we did not study these further, they could be useful for future studies. These data suggest that drugs that improve stress resistance in mouse fibroblasts may also increase Fmo levels.

Based on this result, we hypothesized that some of these compounds may also induce Fmo genes in other organisms, and that this induction could benefit the long-term health of a whole organism. Considering the low throughput, high cost, and slow pace of lifespan studies in mice, we chose to study the top 80 drug hits for stress resistance from Lombard et al. in *C. elegans* to see if they would induce Fmos and if so, increase longevity (Fig. 1F).

Since *fmo-2* is a conserved longevity gene identified in *C. elegans*, we first measured *fmo-2* induction in *C. elegans* using the transcriptional reporter *fmo-2p::mCherry*. *C. elegans* can be refractory to

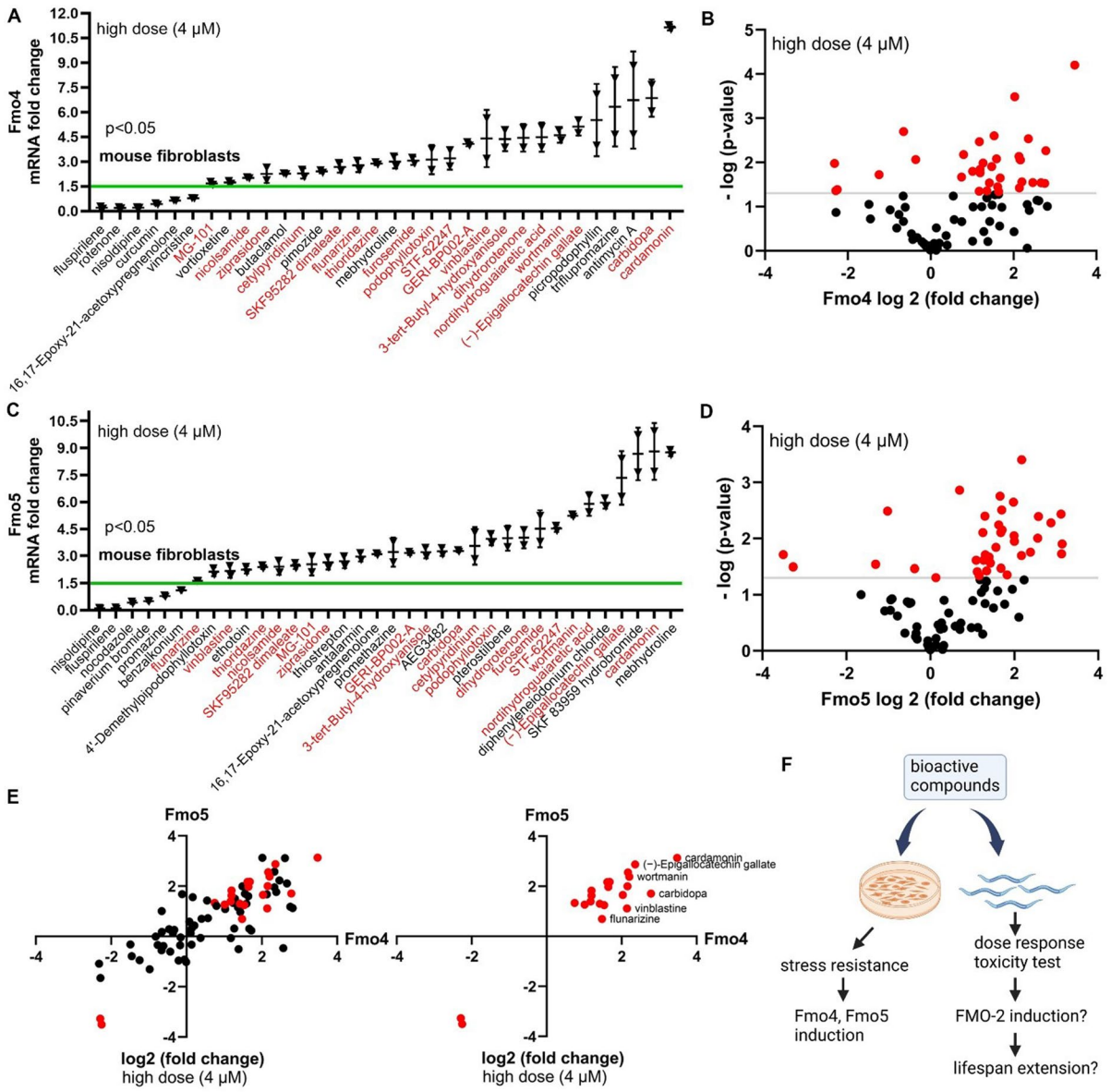

Fig. 1 Drugs that increase stress resistance in mouse fibroblasts also increase *Fmo4* and *Fmo5* transcript levels. **A**–**D** Changes in expression of *Fmo4* and *Fmo5* mRNA in mouse fibroblasts from UM-HET3 mice treated with 4 μM of the indicated drugs compared to DMSO control. *Fmo4* or *Fmo5* mRNA levels were measured by qRT-PCR. Horizontal lines represent the mean, and error bars represent SD. Drugs that increase both *Fmo4* and *Fmo5* mRNA levels are shown in red in **A** and **C**. The *x*-axis values, shown on a log2 scale in **B** and **D**, represent the change of mRNA levels. The *y*-axis values, shown on a −log10 scale in **B** and **D**, represent the *P*-values. Drugs that affect the mRNA levels of *Fmo4* or *Fmo5* significantly are shown in red in **B** and **D**. **E** Drugs that co-regulate mRNA levels of *Fmo4* and *Fmo5* are shown by a scatter plot on a log2 scale fold change. Drugs that significantly increase both *Fmo4* and *Fmo5* mRNA levels are shown in red in the second quadrant. **F** Diagram showing that bioactive compounds increase stress resistance and induce *Fmo4* and *Fmo5* levels in mouse fibroblasts and will be tested for *fmo-2* induction and lifespan extension in *C. elegans*. All drugs shown have $P < 0.05$ when compared to control (Welch two-sample *t*-test, two-sided)

small molecules [19]. Therefore, we first tested each compound for toxicity over 24 h in a wide dose range. Using toxicity data, we began treatment of the reporter animals using the highest dose that did

not lead to any death in toxicity tests (all doses were between 1 μM and 1 mM) (Supplementary Table 4). We chose the highest nontoxic dose because we wanted the best possibility that a compound would get into the worms and potentially induce *fmo-2*. We assumed that these high doses might not be ideal for lifespan but would give us the highest number of compounds that could induce *fmo-2* at any dose (Supplementary Table 4). PFA-killed bacteria were used as the food source to minimize metabolism of the drugs by live bacteria [20]. Using this methodology, the resulting data show that 19 of the 80 tested drugs *significantly* ($P < 0.05$) increase *fmo-2* expression, and 10 of these induce *fmo-2* more than twofold (Fig. 2A–B). We previously reported the serotonin antagonist mianserin induces *fmo-2* by approximately 2-fold [21] (Fig. 2). We used mianserin-treated worms as a cut-off threshold between strong hits (> twofold induction) and weak hits (< twofold but > 1.5-fold) (Fig. 2C–D). Thirteen of the FMO inducers in mouse fibroblasts also induced *fmo-2* in *C. elegans*, including butaclamol, thioridazine, trifluoperazine, dihydrorotenone, and diphenyleneiodonium among the strong hits and MG-101, flunarizine, furosemide, vinblastine, picropodophyllin, astemizole, promethazine, and AEG3482 among the weak hits (Fig. 1; Fig. 2). To test whether the 80 stress resistance-inducing compounds are enriched for *fmo-2* induction, we performed a power analysis and under the assumption that no more than 5% of random compounds would induce *fmo-2*. To reach 80% power and $P \leq 0.05$ for statistical significance of the enriched drug hits (~25% enrichment of 19 hits from 80 compounds), 12 to 18 random compounds need to be tested (Fig. S2**F**). We therefore tested 16 randomly selected drugs that did not induce stress resistance in the previous report [9]. The results showed that none of the 16 drugs increased *fmo-2* induction at 3 doses, supporting enrichment of *fmo-2* induction among stress resistance-inducing drugs (Fig. S2). Together, our data show that nearly 25% of the drug hits that improve stress resistance in mouse fibroblasts induce FMO in both mouse cells and *C. elegans*.

fmo-2-inducing drugs extend lifespan in a dose-dependent manner

Since stress resistance and lifespan extension are often positively correlated and *fmo-2* overexpression is sufficient to extend lifespan in *C. elegans*, it is plausible that *fmo-2* inducers that increase oxidative stress resistance in mouse fibroblasts could promote longevity in nematodes. To test this hypothesis, we applied a dose range of four concentrations of each *fmo-2* inducer to *C. elegans* wild-type N2 worms and examined lifespan after drug treatments (Fig. 3; Fig. S3**;** Supplementary Tables 3 and 4). Considering lifespan measurement is a long-term assay while *fmo-2* induction is a short-term assay with overnight treatment, we used the single drug concentration that induced *fmo-2* shown in Fig. 2 as the highest dose in the range of four different doses applied to worms for the lifespan assay. Interestingly, with the exception of chlorhexidine, all of the strong *fmo-2* inducers extended lifespan at multiple doses tested within the dose range (Fig. S3). The best dose that extends lifespan for each *fmo-2* inducer is shown in Fig. 3. To test for the robustness of our results, we also validated our lifespan results for a subset of compounds (thioridazine, trifluoperazine, methylbenzethonium, diphenyleneiodonium, and chlorhexidine) using a robotic imaging system designed for automated measurement of *C. elegans* lifespan and health span at a different institution (Fig. S4). Healthspan was measured by the motility of *C. elegans*, which was defined as the last day a worm can move a full body length in the automated measurement. The results are consistent with the manually scored lifespans in that all the drugs tested except chlorhexidine extended lifespan and healthspan of wild-type *C. elegans* (Fig. S4; Fig. 3). These results indicate that *fmo-2* induction is a valuable surrogate for longevity in *C. elegans*, and *fmo-2* level is an accurate marker for lifespan extension.

fmo-2 is required for lifespan extension by *fmo-2*-inducing drugs

Considering that we identified the lifespan extending compounds from Fig. 2 through their induction of *fmo-2*, we hypothesized that they would require *fmo-2* for their lifespan extension. We therefore tested whether lifespan extension by *fmo-2*-inducing drugs requires *fmo-2*. We administered *fmo-2*-inducing drugs to wild-type (N2) or *fmo-2 (ok2147)* knockout animals and measured lifespans. The results, analyzed by cox regression, showed that the *fmo-2* knockout genotype significantly interacts with the drug to abrogate lifespan

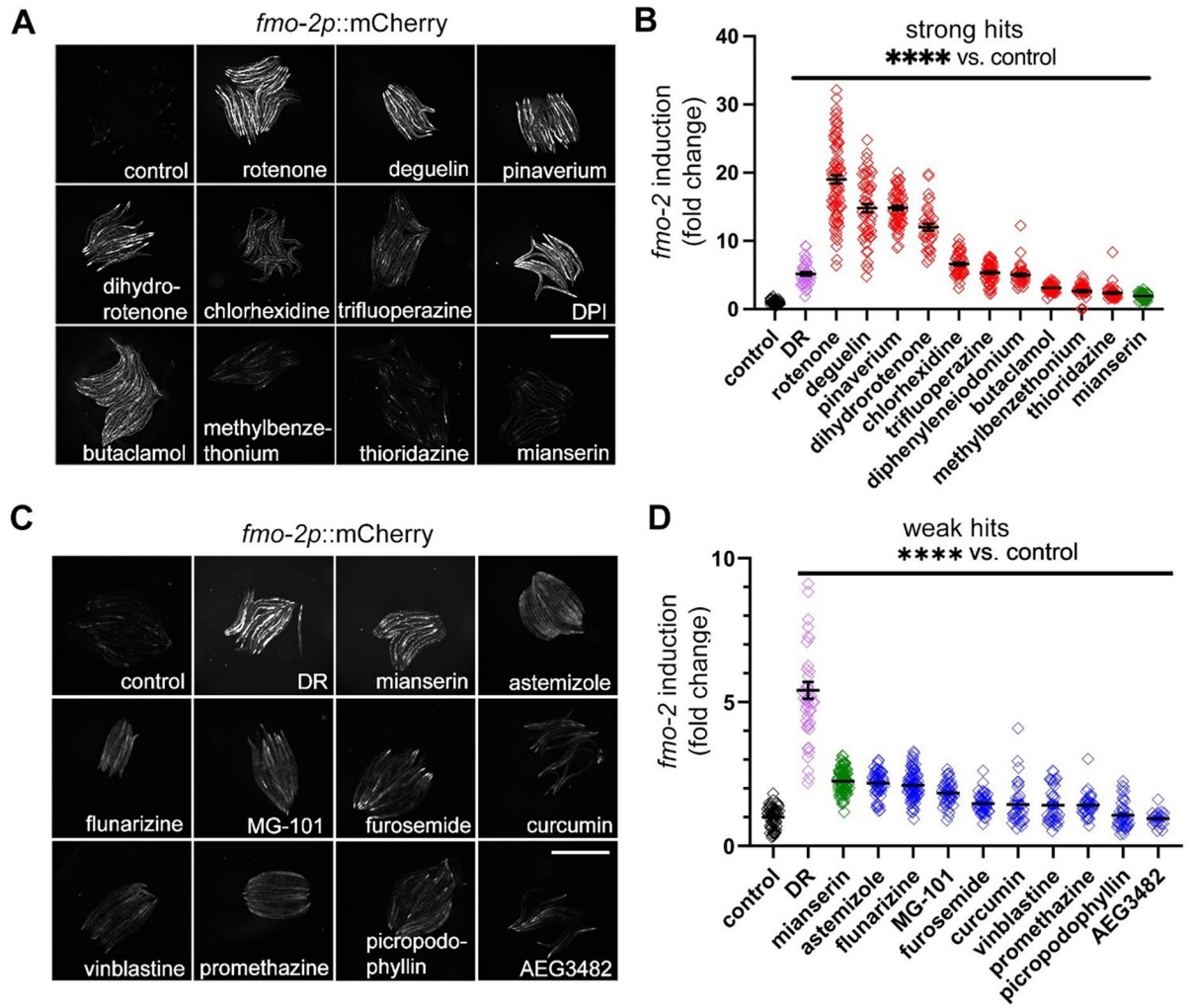

Fig. 2 Ten strong and nine weak *C. elegans fmo-2* inducers are identified from the 80 primary hits that increase stress resistance in mouse fibroblasts. Images and quantification of *fmo-2p::mCherry* after drug treatments. Strong hits (**A**–**B**, red) are defined as drugs that induce *fmo-2* more than mianserin (as a cut-off threshold shown in green). Weak hits (**C**–**D**, blue) are those agents that induce *fmo-2* more than 1.5-fold but less than mianserin dose (green). Dietary restriction (DR) condition is a positive control that induces *fmo-2* (purple). Fluorescence intensity in **A** cannot be compared to intensity in **C**, since they were performed and analyzed in different experiments with different exposure times. Worms were treated with 1-µM rotenone, 100-µM deguelin, 100-µM pinaverium bromide (pinaverium), 100-µM dihydrorotenone, 30-µM chlorhexidine, 100-µM trifluoperazine, 500-µM diphenyleneiodonium (DPI), 500-µM butaclamol, 100-µM methylbenzethonium, 100-µM thioridazine for strong hits; 100-µM mianserin (~twofold induction) as a cut-off threshold between strong hits (>twofold induction) and weak hits (<twofold but>1.5-fold); 1-mM astemizole, 1-mM flunarizine, 1-mM MG-101, 1-mM furosemide, 0.5-mM curcumin, 1-mM vinblastine, 0.5-mM promethazine hydrochloride, 1-mM picropodophyllin, or 1-mM AEG3482 for weak hits. Scale bar, 1 mm. ****Indicates $P < 0.0001$ when compared to control worms (Welch two-sample *t*-test, two-sided). Each symbol represents 1 worm, horizontal lines represent means, and error bars represent standard deviation. Each experiment was repeated at least three times. Single dose selected from toxicity tests (Supplementary Table 4) of each drug was used in the experiment

extension in seven of the nine *fmo-2* inducers that extend wild-type lifespan, with the exceptions of deguelin and butaclamol (Fig. 4; Supplementary Table 5). We also observed that *fmo-2* knockout animals were less consistent in their lifespans in comparison to WT, demonstrating either normal or

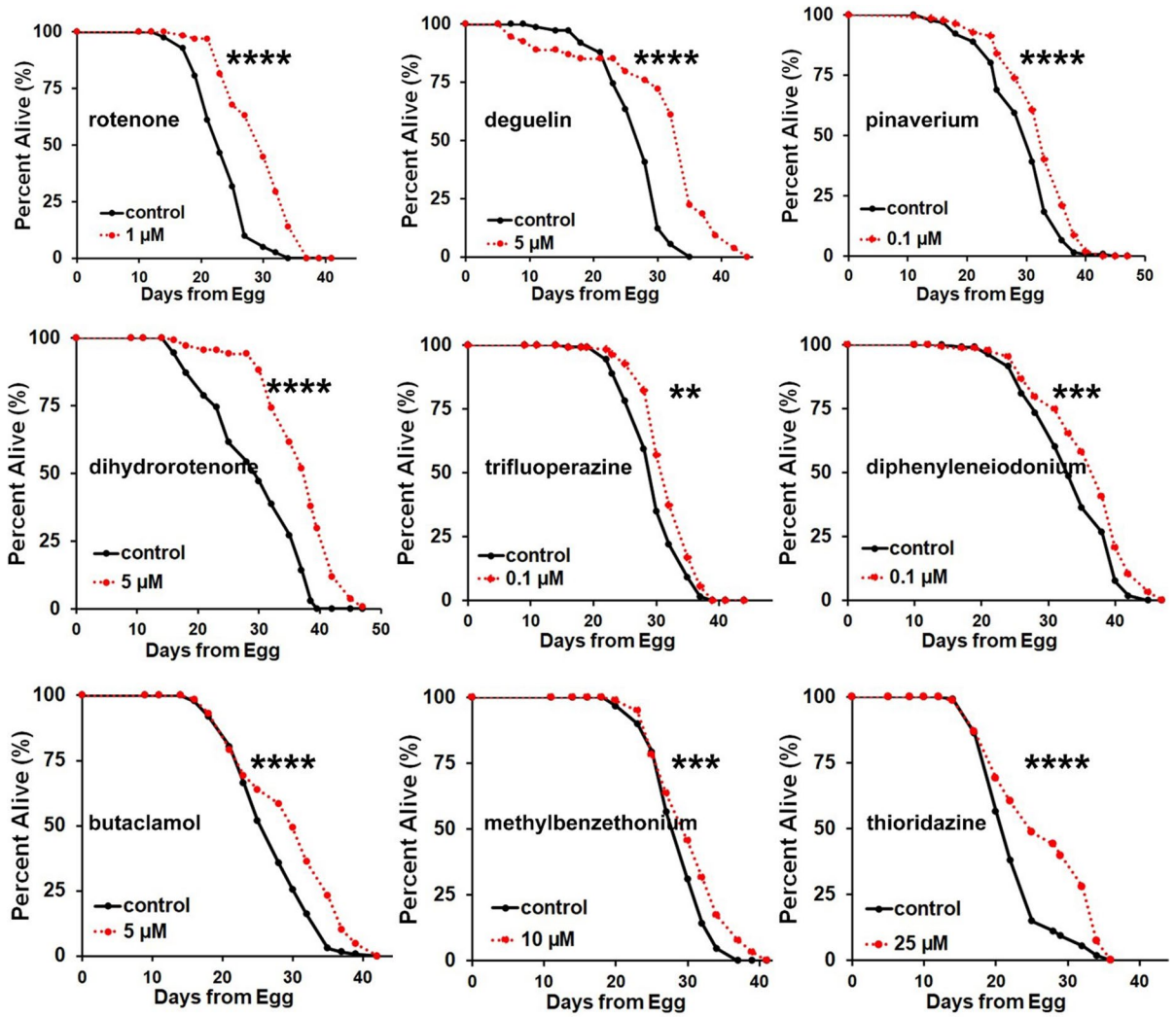

Fig. 3 Nine of ten strong *fmo-2* inducers increase lifespan in *C. elegans*. Survival curves of wild-type *C. elegans* after drug treatments. Lifespans were significantly ($P < 0.05$ by log-rank) extended by the indicated *fmo-2* inducers under the specified concentration. Wild-type *C. elegans* (N2 Bristol) were synchronized to L4 stages, treated with indicated drugs, and then lifespan was measured. ****indicates $P < 0.0001$; ***indicates $P < 0.001$; **indicates $P < 0.01$ when compared to control treated worms (log-rank test). *P*-values (log-rank test), lifespan replicates, and lifespan statistics are listed in Supplementary Table 3. Each lifespan was performed at least two times with multiple doses. The best dose was performed at least four times, with one replicate shown here

shortened lifespan. However, there is no obvious correlation between *fmo-2* KO lifespan compared to WT and whether *fmo-2* is required for drug-mediated longevity. Taken together, these results suggest that *fmo-2* is required for most of these drugs to promote longevity.

Mitochondrial complex I inhibitors induce *fmo-2* and extend lifespan through the HIF-1 signaling pathway

Since the increase of longevity by hypoxia and HIF-1 requires *fmo-2*, we next investigated whether any of these *fmo-2* inducers act via the HIF-1

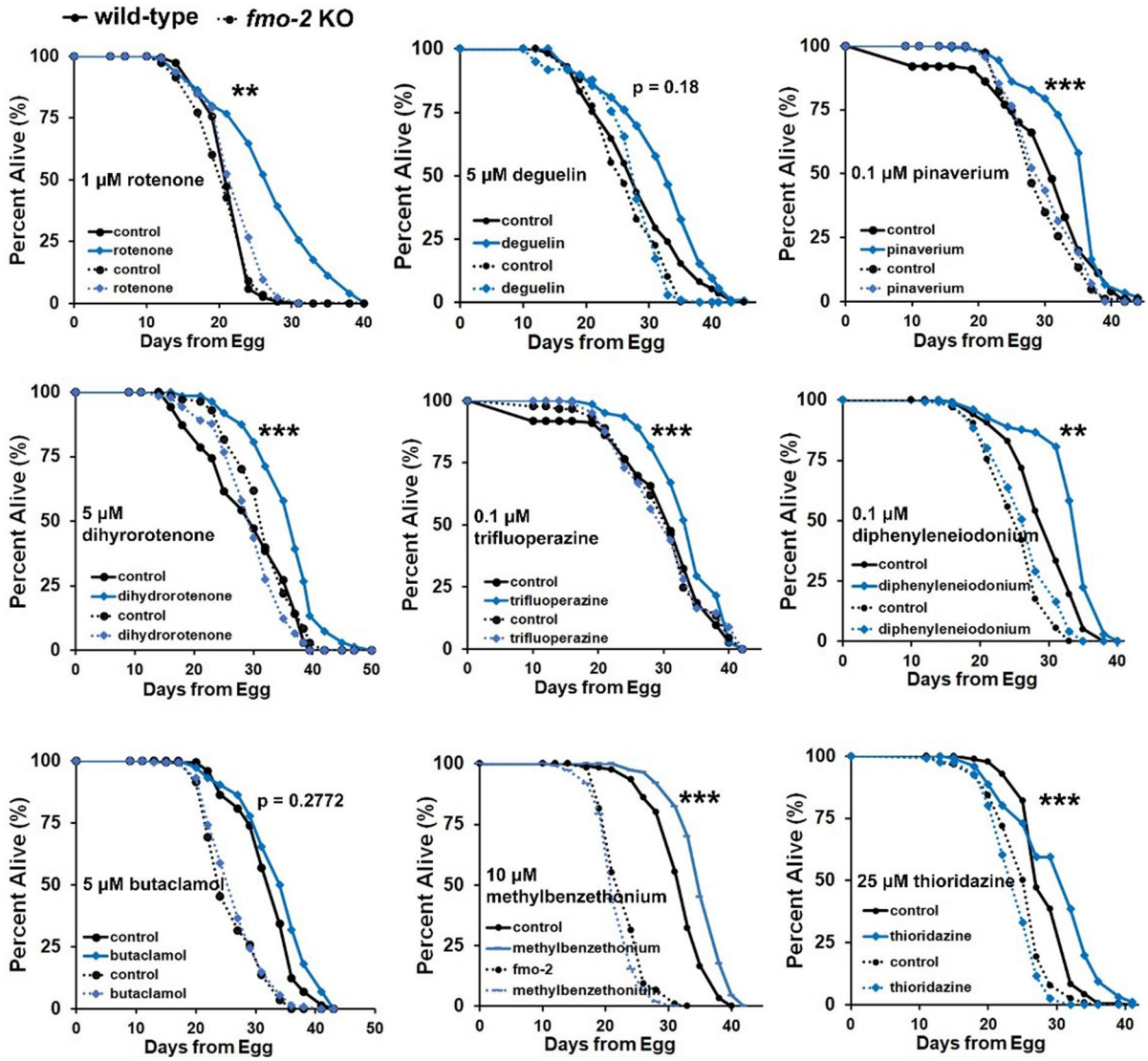

Fig. 4 *fmo-2* is required for *fmo-2* inducers to increase lifespan in *C. elegans*. Survival curves of wild-type (N2 Bristol) or *fmo-2 (ok2147)* knockout animals after drug treatment. Lifespan extension by seven of nine of these drugs is significantly dependent on *fmo-2*. N2 and *fmo-2* knockout strains were synchronized at L4 stages, treated with indicated drugs, and then lifespan was measured. ***indicates $P < 0.001$; **indicates $P < 0.01$ when drug induced lifespan extension of wild-type strain compared to *fmo-2* strain (cox regression). *P*-values (log-rank test) and Cox regression lifespan analyses are listed in Supplementary Tables 3 and 5

signaling pathway. To test this, we generated a *fmo-2p::mCherry* transcriptional reporter in the *egl-9(sa307)* mutant background. EGL-9 is an oxygen-dependent enzyme that hydroxylates HIF-1, rendering HIF-1 less active and allowing for its recognition by the E3 ligase VHL-1. Under normoxia, VHL-1 ubiquitinates hydroxylated HIF-1 and targets it for degradation. In *egl-9(sa307)* mutants, hydroxylation of HIF-1 is impaired, leading to HIF-1 stabilization that serves as a genetic mimic of a hypoxic environment. *fmo-2* is highly induced in *egl-9* mutant worms (Fig. S5**A**). Drugs that strongly increased *fmo-2* (see Fig. 3) were therefore tested in the *egl-9* mutant strain to see whether these drugs further induce *fmo-2*. The results show that mitochondrial complex I inhibitors rotenone and dihydrorotenone do not further induce

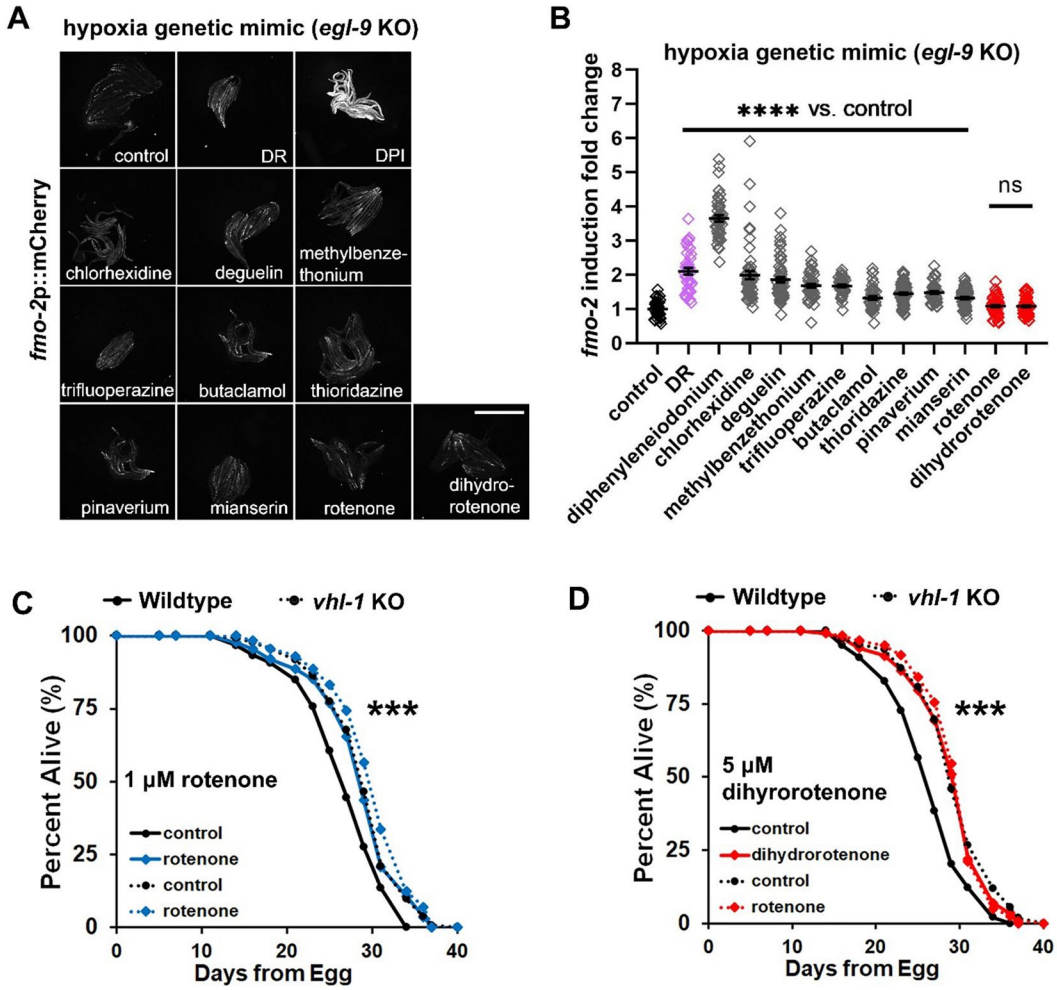

Fig. 5 Mitochondrial complex I inhibitors induce *fmo-2* and extend lifespan within the hypoxia pathway. **A**–**B** Images and quantification of *fmo-2p::mCherry* by strong drug hits in the *egl-9* mutant background. Red denotes drugs that do not further induce *fmo-2*, while gray denotes significant additional induction of *fmo-2* in the *egl-9* mutant. Dietary restriction (DR) condition is a positive control that induces *fmo-2* (purple). In all experiments, *fmo-2*p*::mCherry;egl-9(sa307)* animals were synchronized to L4 stage before treatment with the indicated drugs. Worms were treated with 1-µM rotenone, 100-µM deguelin, 100-µM pinaverium bromide, 100-µM dihydrorotenone, 30-µM chlorhexidine, 100-µM trifluoperazine, 500-µM diphenyleneiodonium (DPI), 500-µM butaclamol, 100-µM methylbenzethonium, 100-µM thioridazine, and 100-µM mianserin as a positive control. Scale bar, 1 mm. **C**–**D** Survival curves of *vhl-1* knockout strains treated with 1-µM rotenone or 5-µM dihydrorotenone from L4 stage. Rotenone and dihydrorotenone do not significantly extend lifespan of *vhl-1(ok161)* worms. ****indicates $P < 0.0001$ when compared to control (Welch two-sample *t*-test, two-sided) in **B**. ***indicates $P < 0.001$ when drug induced lifespan extension of wild-type strain compared to *vhl-1* strain (Cox regression) in **C** and **D**. *P*-values (log-rank test) and Cox regression analyses of lifespan statistics are listed in Supplementary Tables 3 and 5

fmo-2 in the *egl-9* mutant strain, which indicates that these two drugs likely induce *fmo-2* in the HIF-1 signaling pathway (Fig. 5A–B).

To further test whether rotenone and dihydrorotenone extend lifespan in the HIF-1 signaling pathway, we combined these drugs with the lifespan extending *vhl-1* knockout strain. We used the *egl-9* mutant strain for the fluorescent induction experiments due to its stronger induction of fluorescence in the *fmo-2p::mCherry* background, but because *egl-9* mutant has pleiotropic effects that limit its effect on lifespan [22], we used the *vhl-1(ok161)* strain for lifespans. *vhl-1* mutants have similar stabilization of HIF-1 to *egl-9* mutants; only HIF-1 is hydroxylated,

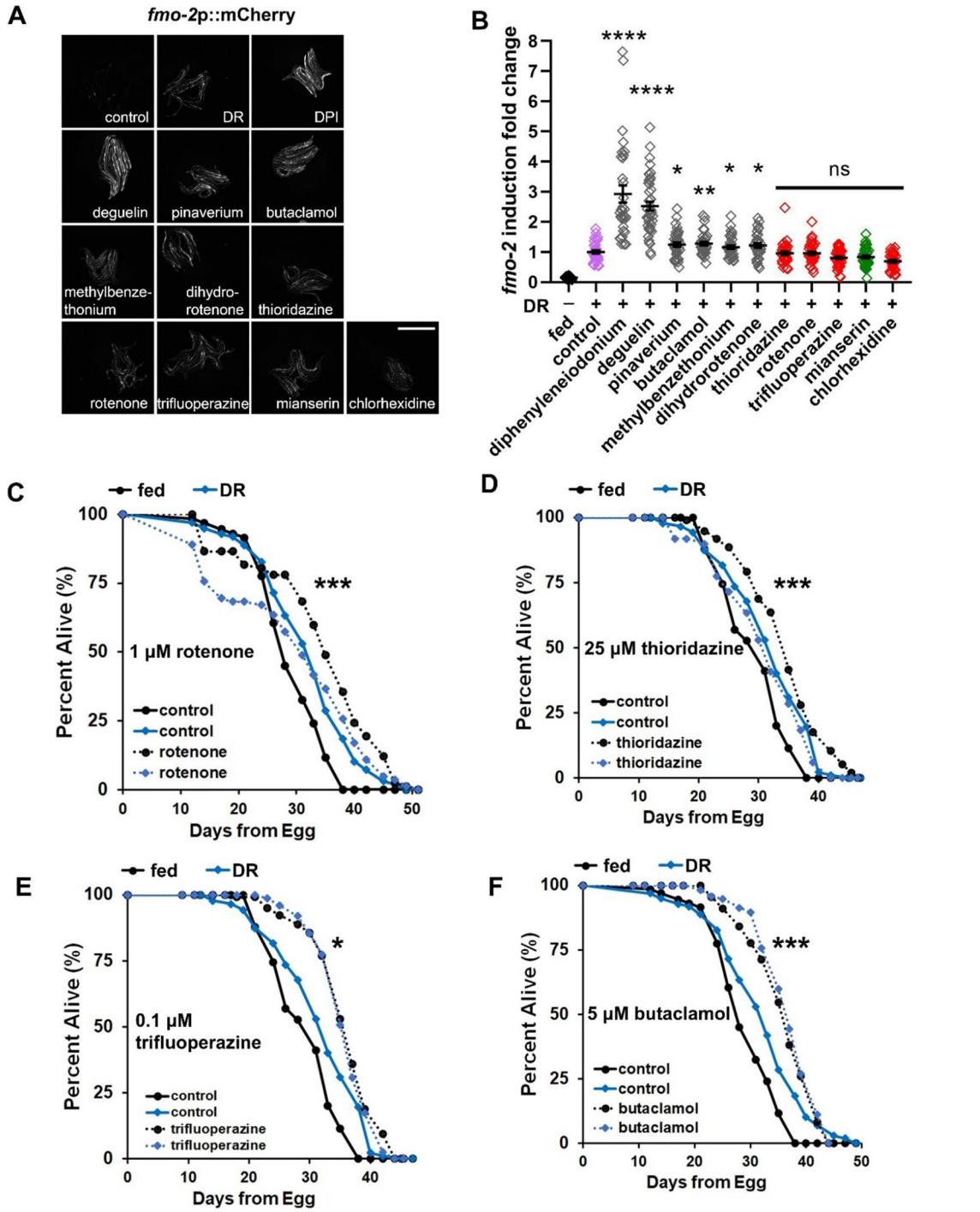

and its activity is modified and/or limited [23–25]. Loss of *vhl-1* also leads to a robust increase in lifespan that is dependent upon HIF-1 and FMO-2 [10] (Fig. 5C–D). The combination of *vhl-1* with rotenone or dihydrorotenone show that drug treatment does not further extend lifespan of *vhl-1* knockout (Fig. 5C–D), supporting their acting in the HIF-1 pathway. To test whether these mitochondrial complex I inhibitors extend lifespan by inhibiting mitochondrial respiration, we also applied these drugs to

◂**Fig. 6** Dopamine D2 receptor antagonists and rotenone induce and extend lifespan in the DR pathway. **A–B** Images and quantification of *fmo-2p::mCherry* induction by strong drug hits under DR condition. Drugs that do not further induce *fmo-2* are in red, while drugs that further induce are in gray. The DR condition (without drug treatment) is in purple. All *fmo-2p::mCherry* animals were synchronized to L4 stage and treated with indicated drugs under DR condition for 18 h. Worms were treated with 1-µM rotenone, 100-µM deguelin, 100-µM pinaverium bromide, 100-µM dihydrorotenone, 30-µM chlorhexidine, 100-µM trifluoperazine, 500-µM diphenyleneiodonium (DPI), 500-µM butaclamol, 100-µM methylbenzethonium, 100-µM thioridazine, and 100-µM mianserin as a control. Scale bar, 1 mm. **C–F** Survival curves of wild-type worms after drug treatments under DR condition. Rotenone and three DRD2 antagonists thioridazine, trifluoperazine, and butaclamol do not further extend lifespan under DR. Wild-type worms were synchronized to L4 stage, treated with 1-µM rotenone, 25-µM thioridazine, 0.1-µM trifluoperazine, or 5-µM butaclamol under DR condition, and lifespan was then measured. ***indicates $P < 0.001$; *indicates $P < 0.05$ when drug induced lifespan extension of worms under DR condition compared to fed condition (Cox regression) in **C–F**. *P*-values (log-rank test) and Cox regression analyses of lifespan curves comparisons were listed in Supplementary Table 3 by log-rank test. ****indicates $P < 0.0001$; **indicates $P < 0.01$; *indicates $P < 0.05$ when compared to control (Welch two-sample *t*-test, two-sided) in **B**

the long-lived *clk-1(qm30)*, coenzyme Q10, mutant strain (Fig. S5**B–E**). The results show that mitochondrial complex I inhibitors further extend the lifespan of long-lived *clk1* mutant, suggesting that these drugs extend lifespan independent of mitochondrial respiration. In summary, these data suggest that mitochondrial respiration complex I inhibitors rotenone and dihydrorotenone induce *fmo-2* and extend lifespan in an overlapping pathway within HIF-1 signaling.

Drugs including dopamine D2 receptor antagonists induce *fmo-2* and extend lifespan through the DR pathway

Since *fmo-2* also mediates effects of DR on longevity, we next investigated whether these *fmo-2* inducers increase *fmo-2* levels and extend lifespan via the DR pathway. To test this, we applied DR to the *fmo-2p::mCherry* transcriptional reporter strain in combination with drug treatments. The results show that rotenone and chlorhexidine do not further induce *fmo-2* under DR (Fig. 6A–B). Similarly, dopamine receptor D2 antagonists thioridazine and trifluoperazine do not further induce *fmo-2* under DR (Fig. 6A–B). It is possible that the dose could be different from the optimal dose of what we have tested in the drug-only *fmo-2* induction (Fig. 2) when the drugs are combined with DR treatment for *fmo-2* induction (Fig. 6A–B). However, with 6 drugs from the 10 *fmo-2* inducers further inducing *fmo-2* under DR as negative controls and previously reported DR mimetics mianserin [21] not further inducing *fmo-2* as a positive control, these results indicate these four drugs interact with the DR pathway and likely induce *fmo-2* within the DR pathway (Fig. 6A–B).

To further test whether these drugs extend lifespan via the DR pathway, we treated dietary restricted worms with rotenone and showed that rotenone does not further extend lifespan of dietary restricted worms (Fig. 6C). Chlorhexidine is the only strong *fmo-2* inducer that does not extend lifespan (Fig. S2); therefore, we did not test whether it further extends lifespan under DR. Thioridazine and trifluoperazine are two other drugs that induce *fmo-2* in the DR pathway (Fig. 6A–B), and both of these are dopamine receptor D2 antagonists. Butaclamol is also a dopamine receptor D2 antagonist that strongly induces *fmo-2* (Fig. 2A–B), but butaclamol did further induce *fmo-2* in DR-treated worms (Fig. 6B). To explore whether antagonizing dopamine receptor could be a common mechanism that overlaps with DR-mediated lifespan extension, we tested all three dopamine receptor D2 antagonists (thioridazine, trifluoperazine, and butaclamol) for their lifespan extension in combination with DR. The results showed that each of the D2 antagonists do not further extend lifespan under DR when compared to drug treatments under fed condition (Fig. 6D–F). In summary, these data suggest that rotenone and dopamine D2 antagonists induce *fmo-2* and extend lifespan in an overlapping pathway within DR.

Together, we find that two drugs induce *fmo-2* and extend lifespan using the hypoxic response-mediated signaling pathway (Fig. 5), and four drugs induce *fmo-2* and extend lifespan using the DR pathway (Fig. 6). Interestingly, rotenone fell into both categories, connecting the hypoxia pathway and DR through mitochondrial complex I inhibition. The other four drugs that induce *fmo-2* and extend lifespan likely act through other mechanisms. Future studies will focus on these mechanisms in addition to the drug targets within the HIF-1 signaling or DR pathway. Collectively, these results suggest that *fmo-2* induction is a useful approach to identify drugs that can extend

lifespan in *C. elegans* and can also provide valuable information about possible mechanisms of action connecting drug effect on *fmo-2* to lifespan effects.

Discussion

Here, we demonstrate an approach to identify drugs that increase *C. elegans* lifespan by Fmo induction. By starting with a relatively narrow list of drugs that improve stress resistance in mouse fibroblasts, we found that 65% of the drugs (52 drugs out of 80) increased either *Fmo4* or *Fmo5* expression significantly under at least one dose. More than 10% of the drugs (12 drugs for *Fmo4* and 8 for *Fmo5*) increase Fmo expression significantly at three doses in mouse fibroblasts. In *C. elegans*, 19 of the 80 stress resistance-promoting drugs induce nematode *fmo-2*, while 0 of 16 random drugs did. This suggests that drugs that improve stress resistance in fibroblasts also increase FMO levels in both mouse fibroblasts and *C. elegans*. We further confirmed that of the top 10 *fmo-2* inducers, 9 extend lifespan in *C. elegans* at one or more doses. We summarize these drugs that induce FMOs in mouse fibroblasts and/or in *C. elegans* and/or extend lifespan in *C. elegans* in Supplementary Table 6. By combining the drug hits with hypoxia or DR to test for *fmo-2* induction in *C. elegans*, we are able to place many compounds into pathways. This shows that *fmo-2* induction can predict lifespan extension and help to place drugs into different longevity pathways. Our data provide a promising longevity indicator that could be developed into a tool for screening compounds for potential longevity benefits.

Our findings show that many drugs that can render mouse cells resistant to stress-mediated death also induce Fmos in mouse cells, in *C. elegans*, or often in both models. Since *fmo-2* plays a necessary role in several lifespan-extending pathways in *C. elegans*, and its overexpression is itself sufficient for worm lifespan extension, it seems plausible that drug-induced Fmo isoforms in one or more tissues could play a role in the pathways by which drugs extend healthy lifespan in mammals, too. Notably, the doses for cultured cells, the doses for nematodes, and the doses for organisms (e.g., mice or humans) will be different and require careful testing to determine. The expected drug concentration in the nematode is often 10–1000 times lower than the applied concentration [26]; thus, concentrations in micromolar doses will often translate to nanomolar doses in mammals. Since Fmos are highly conserved across species, we speculate that high-throughput screens based on induction of Fmo in mouse (or human) cells, or in worms, or in both models in parallel, could provide new drug leads that deserve high priority for testing as antiaging drugs in mice. We acknowledge, however, that the degree of overlap between drugs that induce Fmo expression in mammalian cells and drugs that extend mouse lifespan is currently uncertain. Future work to test the efficacy of these compounds on mice lifespans will provide definite results of the translatability of these *fmo-2* inducers from worms to mammals.

From the primary 80 drug hits that increase stress resistance in mouse fibroblasts, 10 drugs strongly induce *fmo-2*, and 9 of these 10 extend lifespan in *C. elegans*. Four of these 10 drugs are in the category of mitochondrial respiration chain modulators, and 3 of the 10 drug hits are in the category of dopamine D2 antagonists. It has been reported that mitochondria play an essential role in lifespan modulation in *C. elegans* [27, 28]. Consistent with the evidence in mice, the levels of mitochondrial fatty acid β-oxidation enzymes and subunits of mitochondrial oxidative phosphorylation complexes I-IV are upregulated in long-lived mouse models of growth hormone receptor knockout (GHRKO) and Snell dwarf mouse livers [29]. Dopaminergic signaling can also affect long-term health. Dopamine D4 receptor knockout mice display a decrease in lifespan [30]. Loss of function mutant of dopamine D2 receptor DOP-3 blocks lifespan extension by an antihypertensive drug, reserpine, in nematodes [31]. Our recent report also showed that food odor stimulates dopamine release and binding to DOP-3 to block longevity under DR conditions [21]. It will be intriguing to further investigate what genes are targeted by these drug hits in the pathways related to mitochondrial signaling and dopamine signaling in modulating lifespan. Notably, 1 of the 10 drug hits, chlorhexidine, an antiseptic and disinfectant, induces *fmo-2* but does not extend lifespan under the doses of 0.1, 1, 10, and 25 μM in our manually scored lifespan results (Fig. 2; Fig. S3). In the automated lifespan measurement, chlorhexidine does marginally extend lifespan under the doses of 0.01 and 1 μM but not 0.1 μM (Fig. S4). It is possible that its off-target

antiseptic effects separable from *fmo-2* induction contribute to the inconsistent/marginal lifespan benefits from this compound.

The induction of *fmo-2* by these compounds may stem from direct and/or indirect mechanisms downstream of the binding targets of these compounds (e.g., dopamine D2 receptors by dopamine D2 antagonists). Seven of the 9 hit compounds do not extend lifespan in *fmo-2* knockout strains, indicating that, despite of off-target (non-*fmo-2*) possibilities, *fmo-2* is a downstream effector necessary for these drugs to extend lifespan (Fig. 3). However, 2 of the 9 compounds still extend lifespan when *fmo-2* is depleted, indicating that other effector genes in addition to *fmo-2* are likely involved for these compounds to extend lifespan (Fig. 3).

We have demonstrated that among the nine drug hits which induce *fmo-2* and extend lifespan, two drugs act in the hypoxic response mediated signaling pathway (Fig. 5), and four drugs act in the DR pathway (Fig. 6). These results suggest *fmo-2* induction is a useful approach to provide valuable information about possible mechanisms of action connecting drug effects to lifespan effects. The goals of screening pro-longevity drugs through *fmo-2* induction are not to directly identify longevity drugs that will be entered directly into clinical trials, but more to pinpoint drug-targeted mechanisms and pathways to provide targets for the development of more specific pro-longevity drugs with less off-target effects and trade-offs.

Both hypoxia- and DR-mediated longevity involve cell nonautonomous signaling pathways to induce *fmo-2* and extend lifespan [10, 32]. Using *fmo-2* induction as a marker for drug screening and longevity, we expect some of the drugs that extended worm lifespan in our study (Fig. 2A–B; Fig. 3) invoke cell nonautonomous signaling pathways in worms. We previously showed antagonizing serotonin and dopamine signaling induces *fmo-2* and extends lifespan, demonstrating *fmo-2* as a converging downstream effector of serotonin and dopamine signaling for longevity [21]. Future studies will test whether aspects of cell non-autonomous signaling, such as serotonin and dopamine, are required for these drug hits to extend lifespan similar to the signaling required for hypoxia- or DR-mediated longevity [10]. As shown in Fig. 1 and Fig. 2, 13 of the Fmo inducers in mouse fibroblasts also induce *fmo-2* in *C. elegans*, including butaclamol, thioridazine, trifluoperazine, dihydrorotenone, and diphenyleneiodonium in the strong hits; MG-101, flunarizine, furosemide, vinblastine, picropodophyllin, astemizole, promethazine, and AEG3482 in the weak hits. The effects of these drugs on Fmos in mouse cells in culture are almost certainly cell autonomous. It will be intriguing to investigate the cell nonautonomous and autonomous mechanisms of Fmo induction in whole organisms like *C. elegans* and mice as well as in specific tissue microenvironments.

In this study, we focused on the lifespan extending effects of the agents that induce *fmo-2* more than two-fold (Fig. 2A–B; Fig. 3); however, the weak hits and non-hits were not tested for lifespans in this study. Weak hits that induce *fmo-2* significantly but less than two-fold (Fig. 2C–D) could merit testing for longevity effects in worms. It is important to note that there are variations among control lifespans in different batches of experiments due to a myriad of plausible reasons, such as changes in batches of agar, changes in humidity, and different people scoring the experiments. This is true both within and between labs [33]. Therefore, a wild-type control is always included with each individual drug in each individual replicate and run concurrently. We do not compare lifespan data across different drugs or different replicates of the same drug, except in comparison to the WT in each experiment. We note that key experiments were repeated, and results were replicated at a different site, using an automated approach, to ensure robustness. Although there are some variations among wild-type control lifespans between experiments, the relative changes from wild-type control to drug-treated lifespans are consistent (Figs. 3-6). It was reported that one of the weak hits, curcumin, extends lifespan in both *C. elegans* and *D. melanogaster* [34, 35]. Curcumin has been tested by National Institute on Aging Interventions Testing Program (ITP), which evaluates agents for lifespan extension in genetically heterogeneous mice. However, curcumin did not show a significant effect on lifespan of male or female mice at the dose tested [36]. It is also worth noting that rotenone [37], dihydrorotenone [9], and thioridazine [21, 38] were previously reported to extend lifespan in *C. elegans*, consistent with the lifespan extension we show in this work. This serves as additional evidence that this approach is effective, and that *fmo-2* induction uncovered both new and established compounds for lifespan extension.

A high proportion of Fmo inducers in mouse fibroblasts also induce *fmo-2* in *C. elegans*, including 4 drugs (butaclamol, thioridazine, dihydrorotenone, and diphenyleneiodonium) in the 10 strong hits and 8 drugs (MG-101, flunarizine, furosemide, vinblastine, picropodophyllin, astemizole, promethazine, and AEG3482) in the 9 weak hits (Fig. 1; Fig. 2). These data indicate that the translatability of drugs that are screened for *C. elegans fmo-2* induction may be high when tested in the mammalian system. Considering the long lifespan and high cost of mice lifespan studies, there is potential to improve the efficiency of drug discovery and screening by applying pilot screens in *C. elegans* for *fmo-2* induction. This screen of *fmo-2* induction indicated by fluorescent levels can be semiautomated in high-throughput 96-well plates dispensed with drug libraries, followed by fluorescence measurement by high content microcopy. Drug hits from the *C. elegans* screen can be further tested in other systems (e.g., *D. melanogaster*, tissue culture) for lifespan and/or stress resistance, as a lead-up to a limited number of longevity and healthspan tests in mice, and, hopefully, moving a subset toward further development and/or optimization for clinical trials.

Materials and methods

Strains and growth conditions

Standard *Caenorhabditis elegans* cultivation procedures were used as previously described [39, 40]. Briefly, N2 wild type, VC1668 (*fmo-2*(ok2147)), CB5602 (*vhl-1 (ok161)*), MQ130 (*clk-1 (qm30)*), and LZR1 [21] (allele hamSi1) [(pCF150) (*fmo-2*p::mCherry + H2B::GFP) + Cbr-unc-119(+)] II strains were maintained on solid nematode growth media (NGM) fed *Escherichia coli* OP50 throughout life and housed in a 20 °C Percival incubator. All experiments were conducted at 20 °C. Strains used in this study are listed in Supplementary Table 2.

Mouse fibroblasts culture and qPCR

Primary fibroblast cultures were generated using a previously published protocol [41] and studied at the second or third passage. Cells were thawed as needed and passaged twice after thawing. At the second passage, cells were suspended in high-glucose Dulbecco's modified Eagle's medium (DMEM) without sodium pyruvate and supplemented with 10% fetal bovine serum and penicillin/streptomycin/amphotericin B. Cells were kept in a 37 °C, 10% CO_2, and humidified incubator. For qPCR, 0.5×10^6 cells were added to each of four wells in a 6-well plate per sample. Total volume per well was 3 ml (day 1). Cells were left to adhere overnight. On day 2, the compounds were added to the cells, and the cells were left to incubate overnight. On day 3, medium was removed; cells were washed two times with phosphate-buffered saline (PBS). TRIzol was then added directly to the cells, and total RNA was isolated from cells using TRIzol kit (Cat no. 19424, Sigma-Aldrich, Inc., St. Louis, MO, USA) according to the manufacturer's instruction. The RNA was cleaned using the Qiagen RNeasy miniRNA Cleanup Kit (Cat. no. 74204, Qiagen, Valencia, CA, USA). The concentration of total RNA was quantified by measuring the absorbance of RNA sample solutions at 260 nm by using a NanoDrop ND-100. Total RNA (1.0 µg) was reverse transcribed using iScript cDNA reverse transcription kits (Cat. no. 1708891; Bio-Rad, Hercules, CA, USA) according to the manufacturer's instructions. Relative quantities of messenger RNA (mRNA) expression were analyzed using real-time PCR (ABI Prism 7500 Sequence Detection System, Applied Biosystems) with corresponding primers: mGAPDH forward, 5′-gacaactcactcaagattgtcagcaatgc-3′; mGAPDH reverse, 5′-gtggcagtgatggcatggactgtggtc-3′; Fmo4 forward, 5 ′-agcccagcattccacttttg-3′; Fmo4 reverse, 5′-gagagacaagcaggacaggt-3′; Fmo5 forward, 5′-cttcgatggagtcctggtgt-3′; and Fmo5 reverse, 5′-agctcctctcctggtactga-3′. The SYBR (Applied Biosystems) green fluorescence dye was used in this study. Glyceraldehyde-3-phosphate dehydrogenase (GAPDH) was simultaneously assayed as a loading control. The cycle time (CT) was normalized to GAPDH in the same sample. The expression levels of mRNA were reported as fold changes vs. sham control.

PFA-treated food for *C. elegans*

Animals were fed PFA-killed *E. coli* OP50 prepared as previously described [20]. Briefly, a single colony of bacteria was inoculated in Luria broth (LB) and cultured overnight (~ 14 h) in a 37 °C shaker incubator. A total of 32% paraformaldehyde (PFA) was then added to the cultured bacteria (OD_{600} 3.0) to bring the

final concentration to 0.5%. The flask was placed in the 37 °C shaker incubator for 1 h to kill the bacteria. The bacteria were then washed five times to remove any residual PFA. The plates were then seeded with bacteria (OD_{600} 3.0) concentrated 5 × in LB.

Drug treatments

NGM was autoclaved and then cooled to 55 °C prior to the addition of various amounts of test drugs (deguelin (Sigma D0817—5 mg), thioridazine hydrochloride (Sigma T9025—5 g), chlorhexidine (Sigma 282,227—1 g), dihydrorotenone (ChemFaces 6659–45-6), diphenyleneiodonium chloride (Sigma D2926—10 mg), rotenone (Sigma R8875), pinaverium bromide (Toronto Research Chemicals P465000—10 mg), (+)-butaclamol hydrochloride (Santa Cruz SC-252525—5 mg), methylbenzethonium chloride (Sigma M7379—10 g), trifluoperazine hydrochloride (Sigma 46,976—250 mg), flunarizine dihydrochloride (Sigma F8257—1 g), astemizole (Sigma A2861—10 mg), curcumin (Fisher AC218580100—10 g), promethazine hydrochloride (Sigma P4651—25 g), furosemide (Sigma F4381—1 g), AEG 3482 (Fisher 26–511-1—10 mg), vinblastine sulfate salt (Sigma V1377—10 mg), ALLN (Sigma A6185—5 mg), picropodophyllin (Selleckchem 57,668—25 mg), or equal volumes of DMSO/water controls. Compounds dosing for imaging and lifespan assays are summarized in Supplementary Table 4. Fresh batches of plates were poured 1 week before the onset of each experiment and stored at 4 °C protected from light. Plates were seeded with PFA-treated bacteria 2–3 days before the onset of experiments.

Fluorescence microscopy

fmo-2p::mCherry reporter worms were synchronized by a timed egg-lay on NGM plates. The animals ($n = 50$) were allowed to develop and were transferred to test plates on day 1 adults and imaged after 24 h. Microscope slides were prepared 1 h prior to microscopy with a 3% agar mount. The worms were immobilized in 10 µL of 30-mM sodium azide placed on the agar pad. Pictures were taken immediately after slide preparation using a Leica M165FC dissecting microscope. Fluorescence mean comparisons were quantified in ImageJ [42] bundled with 64-bit Java 1.8.0 using polygon tool and saved as macros. Experimental conditions were normalized to DMSO or water controls. Data were plotted by Microsoft Excel 365 and GraphPad Prism.

Lifespan measurements

Synchronization and preparation of animals for lifespan experiments were conducted as previously published [43]. Briefly, 15 gravid adults were placed on new NGM plates. After 4 h, the gravid adults were removed, and the plates with synchronized eggs were placed back in the 20 °C incubator until they reached late L4/young adult (~2.5 days). Animals were transferred to plates with drugs or solvents in the agar, 33 µL of 150-mM fluorodeoxyuridine (FUdR), and 100 µL of 50 mg/mL ampicillin per 100-mL NGM to prevent the development of progeny and growth of contaminating bacteria. Approximately, 60 worms were transferred to test and control plates with PFA-treated concentrated bacteria (5 × from 1×10^9 colony-forming units (CFU) /mL) or diluted bacteria (0.5 × from 1×10^9 CFU /mL) on days 3, 4, 7, and 10 from egg. A minimum of two plates per strain per condition were used per replicate experiment. Experimental animals were scored every 2–3 days and considered dead when they did not move in response to prodding under a dissection microscope. Worms that crawled off the plate were not considered.

Automated lifespan measurements

Plate preparation

Automated *C. elegans* lifespan experiments to validate drug efficacy were conducted at the University of Arizona. Animals were age synchronized by hypochlorite treatment. Briefly, a plate containing gravid adults is washed from a plate with sterile water. Worms were treated twice with 5-mL alkaline hypochlorite solution (1-N NaOH, 0.75% sodium hypochlorite) separated by 2 min of shaking and then rinsed with water. Eggs were resuspended and added to a fresh 6-cm NGM plates seeded with live *E. coli* OP50 bacteria. Synchronized L4 larva were transferred to 6-cm NGM plates containing 50-µM 5-fluorodeoxyuridine (FUdR) and the indicated

concentration of each drug or DMSO and seeded with 10×concentrated live *E. coli* OP50 and transferred to fresh plates on days 2 and 4 of adulthood. On day 7 of adulthood, animals were transferred to WorMotel single-worm culture environments [44] containing drug or DMSO prepared as previously published [45]. For both 6-cm petri plates and WorMotels, drug or DMSO was added to the concentrated bacteria before adding to the plate and allowed to diffuse into the media. Drug concentrations reflect the final total concentration in the plate or WorMotel well.

Automated image collection

Images for automated lifespan and activity analysis were collected essentially as previously published [46]. Briefly, a computer numerical control (CNC) router platform was equipped for darkfield illumination (red LEDs) and a high-resolution (20-MP low-noise CMOS camera) image capture. Starting at day 7 of adulthood and proceeding through end of life for all animals, every 8 h, a series of 25 whole-plate darkfield images were captured for each WorMotel plate at 5-s intervals. Halfway through each image series, worms are exposed to a 5-s pulse of blue light to stimulate movement. Images are used for subsequent processing to estimate lifespan, activity, and health (see below).

Image analysis

Collected images were used to quantify daily activity, lifespan, and health span as previously published [46]. Briefly, each image series was subjected to image registration (FFT/DFT [47], SURF [48], background filtering and noise reduction (Sobel [49] and top-hat-bottom-hat [50] filtering), illumination normalization (cross-image histogram equalization), and machine-learning guided worm identification (YOLOv5L neural networks (https://zenodo.org/records/3983579)) to determine the location of each worm in each image. Activity was estimated by quantifying changes from image to image across each series. Lifespan (last day any activity is detected) and health span (here defined as the last day a worm can move a full body length) were calculated from daily activity data for each animal.

Statistics and reproducibility

Welch two-sample *t*-tests with two-sided analysis were used to derive *P*-values for *fmo-2* induction comparisons. Log-rank test was used to derive *P*-values for lifespan comparisons [51]. Cox regressions were used to determine whether strains and drugs had interaction effects. Lifespan statistics and replicates are listed in Supplementary Table 3 and Supplementary Table 5. All error bars shown in the figures represent the standard error of the mean (SEM) unless otherwise stated.

Data and materials availability

All data needed to evaluate the conclusions in the paper are present in the paper and/or the supplementary materials. Additional data related to this paper are available upon request from the authors.

Acknowledgements We thank David B. Lombard for providing information and insight on the drugs studied here. We acknowledge Faith Carranza-Connors and Stephanie Leiser for input on and analysis of Cox regression.

Author contribution Study conception, SFL and SH. Data analysis and interpretation, SH, SFL, RLC, AT, SB, AB, MBH, MS, RAM, and GLS. Data collection, SH, RLC, AT, SB, AB, MBH, MS, HM, ER, EW, XL, EAG, DD, WP, and JMC. Wrote the manuscript, SH and SFL. All authors contributed to reviewing and editing the manuscript. All authors approved the manuscript.

Funding This work was funded by the Glenn Foundation for Medical Research and NIH grant R01AG075061 to S. F. L.

Declarations

Conflict of interest The authors declare no competing interests.

References

1. Fontana L, Partridge L, Longo VD. Extending healthy life span–from yeast to humans. Science. 2010;328(5976):321–6. https://doi.org/10.1126/science.1172539.
2. Harrison DE, Strong R, Sharp ZD, et al. Rapamycin fed late in life extends lifespan in genetically heterogeneous mice. Nature. 2009;460(7253):392–5. https://doi.org/10.1038/nature08221.

3. Miller RA, Harrison DE, Astle CM, et al. Rapamycin, but not resveratrol or simvastatin, extends life span of genetically heterogeneous mice. J Gerontol A Biol Sci Med Sci. 2011;66(2):191–201. https://doi.org/10.1093/gerona/glq178.
4. Harrison DE, Strong R, Allison DB, et al. Acarbose, 17-α-estradiol, and nordihydroguaiaretic acid extend mouse lifespan preferentially in males. Aging Cell. 2014;13(2):273–82. https://doi.org/10.1111/acel.12170.
5. Harrison DE, Strong R, Alavez S, et al. Acarbose improves health and lifespan in aging HET3 mice. Aging Cell. 2019;18(2):e12898. https://doi.org/10.1111/acel.12898.
6. Ye X, Linton JM, Schork NJ, Buck LB, Petrascheck M. A pharmacological network for lifespan extension in Caenorhabditis elegans. Aging Cell. 2014;13(2):206–15. https://doi.org/10.1111/acel.12163.
7. Snell TW, Johnston RK, Srinivasan B, Zhou H, Gao M, Skolnick J. Repurposing FDA-approved drugs for anti-aging therapies. Biogerontology. 2016;17(5–6):907–20. https://doi.org/10.1007/s10522-016-9660-x.
8. Admasu TD, ChaithanyaBatchu K, Barardo D, et al. Drug synergy slows aging and improves healthspan through IGF and SREBP lipid signaling. Dev Cell. 2018;47(1):67-79.e5. https://doi.org/10.1016/j.devcel.2018.09.001.
9. Lombard DB, Kohler WJ, Guo AH, et al. High-throughput small molecule screening reveals Nrf2-dependent and -independent pathways of cellular stress resistance. Sci Adv. 2020;6:40. https://doi.org/10.1126/sciadv.aaz7628.
10. Leiser SF, Miller H, Rossner R, et al. Cell nonautonomous activation of flavin-containing monooxygenase promotes longevity and health span. Science. 2015. https://doi.org/10.1126/science.aac9257.
11. Lonser RR, Glenn GM, Walther M, et al. von Hippel-Lindau disease. Lancet. 2003;361(9374):2059–67. https://doi.org/10.1016/S0140-6736(03)13643-4.
12. Larsen PL. Aging and resistance to oxidative damage in Caenorhabditis elegans. Proc Natl Acad Sci U S A. 1993;90(19):8905–9. https://doi.org/10.1073/pnas.90.19.8905.
13. Lin YJ, Seroude L, Benzer S. Extended life-span and stress resistance in the Drosophila mutant methuselah. Science. 1998;282(5390):943–6. https://doi.org/10.1126/science.282.5390.943.
14. Murakami S, Salmon A, Miller RA. Multiplex stress resistance in cells from long-lived dwarf mice. FASEB J. 2003;17(11):1565–6. https://doi.org/10.1096/fj.02-1092fje.
15. Harper JM, Wang M, Galecki AT, Ro J, Williams JB, Miller RA. Fibroblasts from long-lived bird species are resistant to multiple forms of stress. J Exp Biol. 2011;214(Pt 11):1902–10. https://doi.org/10.1242/jeb.054643.
16. Huang S, Howington MB, Dobry CJ, Evans CR, Leiser SF. Flavin-containing monooxygenases are conserved regulators of stress resistance and metabolism. Front Cell Dev Biol. 2021;9:630188. https://doi.org/10.3389/fcell.2021.630188.
17. Steinbaugh MJ, Sun LY, Bartke A, Miller RA. Activation of genes involved in xenobiotic metabolism is a shared signature of mouse models with extended lifespan. Am J Physiol Endocrinol Metab. 2012;303(4):E488–95. https://doi.org/10.1152/ajpendo.00110.2012.
18. Swindell WR. Genes and gene expression modules associated with caloric restriction and aging in the laboratory mouse. BMC Genomics. 2009;10:585. https://doi.org/10.1186/1471-2164-10-585.
19. Hunt PR, The C. Elegans model in toxicity testing. J Appl Toxicol. 2017;37(1):50–9. https://doi.org/10.1002/jat.3357.
20. Beydoun S, Choi HS, Dela-Cruz G, et al. An alternative food source for metabolism and longevity studies in Caenorhabditis elegans. Commun Biol. 2021;4(1):258. https://doi.org/10.1038/s42003-021-01764-4.
21. Miller HA, Huang S, Dean ES, et al. Serotonin and dopamine modulate aging in response to food odor and availability. Nat Commun. 2022;13(1):3271. https://doi.org/10.1038/s41467-022-30869-5.
22. Miller H, Fletcher M, Primitivo M, et al. Genetic interaction with temperature is an important determinant of nematode longevity. Aging Cell. 2017. https://doi.org/10.1111/acel.12658.
23. Shen C, Shao Z, Powell-Coffman JA. The Caenorhabditis elegans rhy-1 gene inhibits HIF-1 hypoxia-inducible factor activity in a negative feedback loop that does not include vhl-1. Genetics. 2006;174(3):1205–14. https://doi.org/10.1534/genetics.106.063594.
24. Shao Z, Zhang Y, Powell-Coffman JA. Two distinct roles for EGL-9 in the regulation of HIF-1-mediated gene expression in Caenorhabditis elegans. Genetics. 2009;183(3):821–9. https://doi.org/10.1534/genetics.109.107284.
25. Kruempel JCP, Miller HA, Schaller ML, et al. Hypoxic response regulators RHY-1 and EGL-9/PHD promote longevity through a VHL-1-independent transcriptional response. Geroscience. 2020;42(6):1621–33. https://doi.org/10.1007/s11357-020-00194-0.
26. Evason K, Huang C, Yamben I, Covey DF, Kornfeld K. Anticonvulsant medications extend worm life-span. Science. 2005;307(5707):258–62. https://doi.org/10.1126/science.1105299.
27. Dillin A, Hsu AL, Arantes-Oliveira N, et al. Rates of behavior and aging specified by mitochondrial function during development. Science. 2002;298(5602):2398–401. https://doi.org/10.1126/science.1077780.
28. Zhang Q, Wu X, Chen P, et al. The mitochondrial unfolded protein response is mediated cell-non-autonomously by retromer-dependent Wnt signaling. Cell. 2018;174(4):870-883.e17. https://doi.org/10.1016/j.cell.2018.06.029.
29. Elmansi AM, Miller RA. Coordinated transcriptional upregulation of oxidative metabolism proteins in long-lived endocrine mutant mice. Geroscience. 2023;45(5):2967–81. https://doi.org/10.1007/s11357-023-00849-8.

30. Grady DL, Thanos PK, Corrada MM, et al. DRD4 genotype predicts longevity in mouse and human. J Neurosci. 2013;33(1):286–91. https://doi.org/10.1523/JNEUROSCI.3515-12.2013.
31. Saharia K, Kumar R, Gupta K, Mishra S, Subramaniam JR. Reserpine requires the D2-type receptor. J Biosci. 2016;41(4):689–95. https://doi.org/10.1007/s12038-016-9652-7.
32. Miller HA, Huang S, Schaller ML, et al. Serotonin and dopamine modulate aging in response to food perception and availability. 2021:2021.03.23.436516. 2021/03/23. Accessed 2021/10/13. https://www.biorxiv.org/content/https://doi.org/10.1101/2021.03.23.436516v1
33. Urban ND, Cavataio JP, Berry Y, et al. Explaining inter-lab variance in C. elegans N2 lifespan: making a case for standardized reporting to enhance reproducibility. Exp Gerontol. 2021;156:111622. https://doi.org/10.1016/j.exger.2021.111622.
34. Liao VH, Yu CW, Chu YJ, Li WH, Hsieh YC, Wang TT. Curcumin-mediated lifespan extension in Caenorhabditis elegans. Mech Ageing Dev. 2011;132(10):480–7. https://doi.org/10.1016/j.mad.2011.07.008.
35. Suckow BK, Suckow MA. Lifespan extension by the antioxidant curcumin in Drosophila melanogaster. Int J Biomed Sci. 2006;2(4):402–5.
36. Strong R, Miller RA, Astle CM, et al. Evaluation of resveratrol, green tea extract, curcumin, oxaloacetic acid, and medium-chain triglyceride oil on life span of genetically heterogeneous mice. J Gerontol A Biol Sci Med Sci. 2013;68(1):6–16. https://doi.org/10.1093/gerona/gls070.
37. Schmeisser S, Priebe S, Groth M, et al. Neuronal ROS signaling rather than AMPK/sirtuin-mediated energy sensing links dietary restriction to lifespan extension. Mol Metab. 2013;2(2):92–102. https://doi.org/10.1016/j.molmet.2013.02.002.
38. Petrascheck M, Ye X, Buck LB. An antidepressant that extends lifespan in adult Caenorhabditis elegans. Nature. 2007;450(7169):553–6. https://doi.org/10.1038/nature05991.
39. Kaeberlein TL, Smith ED, Tsuchiya M, et al. Lifespan extension in Caenorhabditis elegans by complete removal of food. Aging Cell. 2006;5(6):487–94. https://doi.org/10.1111/j.1474-9726.2006.00238.x.
40. Smith ED, Kaeberlein TL, Lydum BT, et al. Age- and calorie-independent life span extension from dietary restriction by bacterial deprivation in Caenorhabditis elegans. BMC Dev Biol. 2008;8:49. https://doi.org/10.1186/1471-213X-8-49.
41. Salmon AB, Murakami S, Bartke A, Kopchick J, Yasumura K, Miller RA. Fibroblast cell lines from young adult mice of long-lived mutant strains are resistant to multiple forms of stress. Am J Physiol Endocrinol Metab. 2005;289(1):E23–9. https://doi.org/10.1152/ajpendo.00575.2004.
42. Schneider CA, Rasband WS, Eliceiri KW. NIH Image to ImageJ: 25 years of image analysis. Nat Methods. 2012;9(7):671–5. https://doi.org/10.1038/nmeth.2089.
43. Sutphin GL, Kaeberlein M. Measuring Caenorhabditis elegans life span on solid media. J Vis Exp. 2009(27). https://doi.org/10.3791/1152.
44. Churgin MA, McCloskey RJ, Peters E, Fang-Yen C. Antagonistic serotonergic and octopaminergic neural circuits mediate food-dependent locomotory behavior in Caenorhabditis elegans. J Neurosci. 2017;37(33):7811–23. https://doi.org/10.1523/JNEUROSCI.2636-16.2017.
45. Gardea EA, DeNicola D, Freitas S, et al. Long-term culture and monitoring of isolated Caenorhabditis elegans on solid media in multi-well devices. J Vis Exp. 2022(190). https://doi.org/10.3791/64681.
46. Freitas S. Worm Paparazzi – a high throughput lifespan and healthspan analysis platform for individual Caenorhabditis elegans. Tucson, AZ, USA: University of Arizona; 2021.
47. Davuluru VSP, Hettiarachchi DLN, Balster E. Performance analysis of DFT and FFT algorithms on modern GPUs. TechRxiv. https://doi.org/10.36227/techrxiv.20264424.v12022.
48. Bay H, Ess A, Tuytelaars T. Gool LV. Speeded-up robust features (SURF). Comput Vis Image Und. 2008;110(3). https://doi.org/10.1016/j.cviu.2007.09.014.
49. Chen W, Yu YJ, Shi H. An improvement of edge-adaptive image scaling algorithm based on Sobel operator. In: In 4th International Conference on Information Science and Control Engineering (ICISCE). 2017. https://doi.org/10.1109/ICISCE.2017.48.
50. Kushol R, Kabir MH, Salekin MS, Rahman ABMA. Contrast enhancement by top-hat and bottom-hat transform with optimal structuring element: application to retinal vessel segmentation. Image Analysis and Recognition. 2017. https://doi.org/10.1007/978-3-319-59876-5_59.
51. Han SK, Lee D, Lee H, et al. OASIS 2: online application for survival analysis 2 with features for the analysis of maximal lifespan and healthspan in aging research. Oncotarget. 2016;7(35):56147–52. https://doi.org/10.18632/oncotarget.11269.

Publisher's Note Springer Nature remains neutral with regard to jurisdictional claims in published maps and institutional affiliations.

Springer Nature or its licensor (e.g. a society or other partner) holds exclusive rights to this article under a publishing agreement with the author(s) or other rightsholder(s); author self-archiving of the accepted manuscript version of this article is solely governed by the terms of such publishing agreement and applicable law.